17. P. Bouverot, *Adaptation to Altitude-Hypoxia in Vertebrates* (Springer-Verlag, Berlin, 1985).
18. K. J. Gaston, *The Structure and Dynamics of Geographic Ranges* (Oxford Univ. Press, Oxford, 2003).
19. We estimate PIO_2 rather than PO_2, because the addition of respiratory water vapor reduces the partial pressure of O_2 in the lung (*20*).
20. See supporting data on *Science* Online.
21. Estimates of maximum altitudes for the Late Permian and Triassic are somewhat low because warm temperatures would have elevated barometric pressure at altitude. However, the impact on O_2 would have been small: Substituting PO_2 and temperature estimates in the hypsometric equation demonstrates that our altitudinal estimates for the Triassic O_2 low (Fig. 1C) underestimate actual limits by at most 0.1 km (*22*). Similarly, our estimates of maximum altitudes in the cold mid-Permian (Fig. 1C) overestimate actual limits by at most ~0.2 km (*22*). Because these effects are relatively small, we ignore them in our simulations.
22. D. Battisti, personal communication.
23. C. C. Labandeira, J. J. Sepkoski Jr., *Science* **261**, 310 (1993).
24. M. R. Frazier, H. A. Woods, J. F. Harrison, *Physiol. Biochem. Zool.* **74**, 641 (2001).
25. K. J. Greenlee, J. F. Harrison, *J. Exp. Biol.* **207**, 497 (2004).
26. D. H. Janzen, *Am. Nat.* **101**, 233 (1967).
27. I. A. Hanski, *Metapopulation Ecology* (Oxford Univ. Press, Oxford, 1999).
28. A. Hallam, P. B. Wignall, *Earth Sci. Rev.* **48**, 217 (1999).
29. M. L. Rosenzweig, *Species Diversity in Space and Time* (Cambridge Univ. Press, Cambridge, 1995).
30. D. B. Rowley, R. T. Pierrehumbert, B. S. Currie, *Earth Planet. Sci. Lett.* **88**, 253 (2001).
31. K. Angielczyk, personal communication.
32. W. J. Hillenius, J. A. Ruben, *Physiol. Biochem. Zool.* **77**, 1019 (2004).
33. C. A. Sidor *et al.*, *Nature*, in press.
34. P. M. Rees, *Geology* **30**, 827 (2002).
35. P. B. Wignall, M. J. Benton, *J. Geol. Soc. London* **156**, 453 (1999).
36. R. A. Berner, *Geochim. Cosmochim. Acta*, in press.
37. R. A. Berner, Z. Kothavala, *Am. J. Sci.* **301**, 182 (2001).
38. We thank R. Berner for providing data, advice, and discussion; K. Angielczyk, M. Benton, R. Buick, C. Carey, T. Daniel, R. Dudley, D. Erwin, J. Graham, T. Hornbein, D. Rowley, J. Ruben, A. Smith, M. Stoeck, and J. West for discussion; D. Battisti for computing the impact of temperature on critical altitudes; and D. Rowley and G. Wang for calculating hypsometric data. Supported by NSF grant IBN-0416843 (R.B.H.) and the NASA Astrobiology Institute (University of Washington Node, P.D.W., principal investigator).

Supporting Online Material
www.sciencemag.org/cgi/content/full/308/5720/398/DC1
Materials and Methods
Figs. S1 and S2
References

29 November 2004; accepted 15 February 2005
10.1126/science.1108019

Open-System Coral Ages Reveal Persistent Suborbital Sea-Level Cycles

William G. Thompson*† and Steven L. Goldstein

Sea level is a sensitive index of global climate that has been linked to Earth's orbital variations, with a minimum periodicity of about 21,000 years. Although there is ample evidence for climate oscillations that are too frequent to be explained by orbital forcing, suborbital-frequency sea-level change has been difficult to resolve, primarily because of problems with uranium/thorium coral dating. Here we use a new approach that corrects coral ages for the frequently observed open-system behavior of uranium-series nuclides, substantially improving the resolution of sea-level reconstruction. This curve reveals persistent sea-level oscillations that are too frequent to be explained exclusively by orbital forcing.

The idea that Quaternary climate cycles are linked to changes in Earth's orbit is central to climate change theory (*1*). The primary evidence for this comes from the marine oxygen isotope ($\delta^{18}O$) record (*2*) and early dating of coral terraces (*3*). However, there is abundant evidence for abrupt climate change that was too frequent to be explained by orbital changes (*4*). Here we attempt to reconstruct sea level between 70 and 240 thousand years ago (ka) with a resolution sufficient to detect suborbital-frequency oscillations, using a new approach to U/Th coral dating (*5*). Several recent lines of evidence suggest that sea level may be more variable than previously thought. An example is the conversion, via a hydraulic model, of a salinity record from the Red Sea into a sea-level curve for the past 470 thousand years (ky) (*6*). This record suggests fairly large (~35 m) suborbital-frequency sea-level changes during glacial periods such as marine isotope stage 3 (MIS 3) and more modest (~15 m) changes during interglacials (for example, during MIS 5). This new Red Sea record augments a growing body of evidence for suborbital sea-level fluctuations in coral records. At the Huon Peninsula of Papua New Guinea, multiple coral terraces were formed during MIS 3, with highstands occurring about every 6 ky (*7*, *8*). There are also more Huon terraces associated with MIS 5 than can be accounted for by orbital variability (*9*). Such evidence is not restricted to New Guinea; closely spaced terraces on Barbados suggest suborbital period changes in sea level during MIS 5a and MIS 5c (*9*, *10*).

The construction of a high-resolution sea-level record requires a large number of accurate coral ages from a limited geographic area, and this has not been possible with standard dating methods. The conventional equations for U/Th age determination (*11*) require that loss or gain of U and Th have not occurred except by radioactive decay after coral death. This closed-system requirement is often violated in fossil corals as a result of the alpha-recoil mobility of U-series nuclides (*12*), and an initial coral $^{234}U/^{238}U$ ratio that is significantly different from that of modern seawater is taken as evidence of open-system behavior and an unreliable age (*13*). Building on earlier attempts to correct for open-system behavior (*14*), we have derived a set of decay equations that corrects coral ages for these effects (*5*). Although conventional U-series coral ages from a single stratigraphic level often differ substantially, open-system ages of these corals are in much better agreement (Fig. 1, A to C), which illustrates the dramatic improvement in the accuracy of coral ages achieved through open-system dating. It has long been known that many conventional coral ages are unreliable, prompting screening for open-system effects (*13*). Such screening improves accuracy but often results in the rejection of up to 90% of measured ages, degrading the resolution of sea-level reconstructions (fig. S1, A and B). By recovering accurate ages for most corals, the open-system method greatly improves the resolution of the resulting record (fig. S1C).

We have constructed (*15*) a high-resolution uplift-corrected sea-level curve for Barbados (Fig. 2), with open-system ages calculated from published isotope ratio data (*5*, *13*, *16*, *17*) and other measurements (table S1). Corals defining this curve are almost entirely *Acropora palmata*, a reef-crest species. An average data density approaching one age per 1000 years during MIS 5 highstands and one age per 2500 years during MIS 7 (to 220 ka) resolves sea-level fluctuations occurring over a few thousand years. For the most part, clearly separated peaks constrained by multiple coral ages define the oscillations characterizing suborbital sea-level variability. However, in mid-MIS 7, between 200 and 220 ka, three potential sea-level peaks are poorly resolved because of overlapping error envelopes. The best constrained portion of the sea-level curve is during MIS 5c, where minor highstands at 100, 103, and 105.5 ka are evident in coral ages from a

Lamont-Doherty Earth Observatory (LDEO) and Department of Earth and Environmental Sciences, Columbia University, Palisades, NY 10964, USA.

*Present address: Department of Geology and Geophysics, 118 Clark Lab, Mail Stop 23, Woods Hole Oceanographic Institution, Woods Hole, MA 02543, USA.
†To whom correspondence should be addressed. E-mail: wthompson@whoi.edu

single outcrop at Salt Cave Point. These three peaks are independently confirmed by coral ages from the University of West Indies and South Point sites. Reproducibility at this level of detail suggests that our method is robust.

We compared our record to four recent sea-level reconstructions from $\delta^{18}O$ records (Fig. 3) that use different approaches to isolate sea level from the other components of the $\delta^{18}O$ signal. At orbital time scales, there is fairly good correspondence between the $\delta^{18}O$ records, which is expected because their chronologies are linked either directly or indirectly to orbital tuning. However, discrepancies between records (for example, during MIS 6) arise from differences in correlation or tuning and illustrate the difficulty of establishing a detailed and precise chronology. Although there are varying degrees of suborbital variability in the $\delta^{18}O$-derived records, it is difficult to find much correspondence between records. This points to the difficulty in extracting the portion of the $\delta^{18}O$ signal that is attributable to sea level and in resolving suborbital variability. Measurement uncertainty and smoothing of the record by bioturbation also limit the resolution of such records. A coral-derived sea-level record is much less ambiguous, because each coral provides a direct sea-level index and a precise radiometric age. Our record resolves the timing and magnitude of the millennial-scale variability that is suggested in some of the $\delta^{18}O$ records.

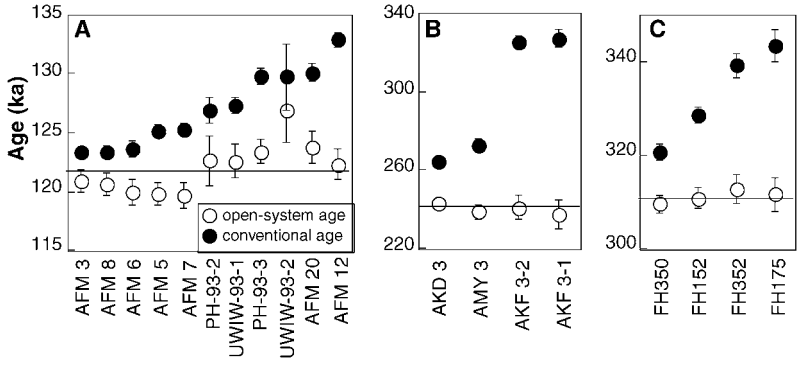

Fig. 1. A comparison of conventional and open-system ages calculated from the same isotope ratio data (*5, 13, 16, 27*). Each group of corals is from a stratigraphically restricted interval, where ages might be expected to be very similar. (**A**) Corals from the top of the University of West Indies terrace, Barbados. (**B**) Corals from the top of St. David's terrace, Christ Church Ridge, Barbados. (**C**) Corals from the 24-m level of the fossil lagoon, Henderson Island, Pacific Ocean.

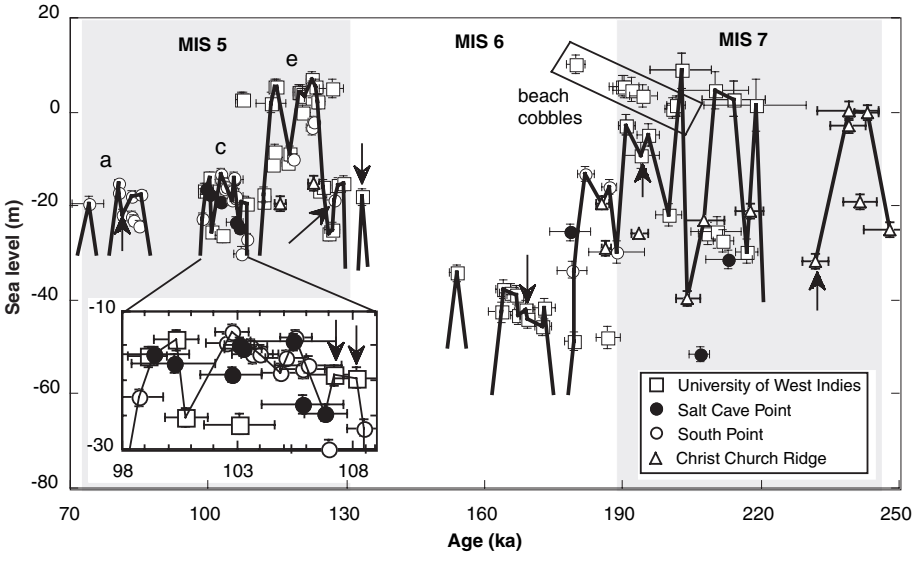

Fig. 2. A high-resolution sea-level curve constructed from Barbados coral data (*5, 13, 16, 17*) using open-system age equations. Plot symbols indicate sample location. Arrows identify the eight corals that are not the reef-crest species *A. palmata*. In general, the sea-level curve is drawn through the highest corals of a given age (*15*). Gaps in the sea-level curve represent large age gaps between closely spaced corals in a single outcrop, where age differences of several thousand years are observed over distances of a few meters. These hiatuses suggest that sea level was lower than the dated strata during these intervals. In all figures, error bars are 2σ and those not visible are smaller than the plot symbols, and MIS boundaries are placed at the orbitally tuned ages of (*28*).

It is useful to compare our record to sea-level and climate records obtained from speleothems (Fig. 4), because U/Th speleothem dating is affected much less by the open-system behavior that disturbs coral ages (*18*). Speleothems recovered from submarine caves provide independent sea-level constraints. Such cave deposits form only when the sea is below the cave's elevation. Therefore, the ages and elevations of such speleothems provide sea-level maxima that should plot above a sea-level curve (Fig. 4A). Although there is some minor conflict with the speleothem data around 200 ka and with a single point during MIS 6 near 165 ka, our sea-level reconstruction is remarkably consistent with these speleothem constraints. Two speleothem data points, at ~130 ka and –50 m, taken together with the coral data, confirm a dramatic oscillation of sea level first indicated by Huon Peninsula corals (*19*) and indicate a minimum sea-level change of >30 m. Furthermore, one speleothem age suggests a minor lowstand in the middle of the broad peak at ~240 ka, which is suggested by the coral data but is not well resolved (Fig. 2). The good agreement of our record with speleothem sea-level constraints provides independent support for the chronology of our sea-level reconstruction. Speleothem growth can also be sensitive to climate change. There are five well-dated records covering the interval under consideration, where the presence or absence of speleothem growth has been linked to climate change. We compared our sea-level reconstruction to these continental speleothem records from Spannagel Cave (Austrian Alps), Clamouse and Villars Caves (France), Newdegate Cave (Tasmania), and several caves in northeastern Brazil (Fig. 4B). In the first four records, speleothem growth ages, indicating a warm and/or wet climate, agree quite well with periods of high sea level. Slowing or cessation of speleothem growth, which are indicative of colder and/or drier climate, correspond to times of lower sea level. The Brazil record, which has been demonstrated to have an antiphase relationship with Greenland temperature, also agrees well with our sea-level record; growth ages (cold Greenland) correspond with times of lower sea level, and brief hiatuses correspond to short-lived sea-level highstands in our record. The good general correspondence of high sea levels with times of warm climate, and lower sea levels with times of colder climate, also increases confidence in our chronology. It is particularly encouraging that several second-order lowstands characterizing suborbital variability in our record correspond closely with independently dated climate reversals documented by hiatuses in speleothem growth (Fig. 4B, arrows).

Our sea-level curve is in good agreement with records we derived from independent coral data. Sea level inferred from Last

Interglacial patch reefs in the Bahamas agrees extremely well with our record (Fig. 5A), indicating two brief highstands at about 125 to 118 ka and 116 to 115 ka. Detailed maps of sample locations combined with open-system ages reveal that these reefs are age-coherent units in stratigraphic order, with the younger reef to seaward. Underlying these patch reefs is a "rubblestone" unit with a wider range of ages that are not in stratigraphic order. This implies that these corals are not in place, although they are reported to be in growth position, which is not unexpected because transported corals have at least a 50% chance of landing upright. This illustrates that open-system ages are useful for distinguishing in situ deposits from transported ones. The stratigraphically inconsistent ages of the rubblestone unit suggest a transgressive beach deposit incorporating older corals from lower stratigraphic levels during storm events, creating the false impression that the Last Interglacial highstand began as early as 127 ka. A substantial fraction of open-system coral ages from Australia also agree well with our record (Fig. 5B), although there is a handful of slightly older corals. Open-system coral ages from an Australian drill core are not in stratigraphic order, suggesting that transported corals may be a problem for this data set as well. Unfortunately, a detailed map of all sample locations is not available to check the stratigraphic consistency of the samples. It is possible that, as in the Bahamas example, the transport of corals from lower stratigraphic levels during storms is extending the apparent duration of the highest sea levels in the Australian record.

An independent sea-level curve for MIS 5a and MIS 5c was constructed using recent Barbados data (Fig. 5C) and the same methods that produced Fig. 2. The detailed reproducibility of minor sea-level changes where data sets overlap in MIS 5c is striking, although the timing of changes during MIS 5a appears slightly different. New data between 80 and 73 ka indicate relatively stable sea level where lower sea levels were inferred from a data gap in our record, suggesting that further work is needed to resolve the discrepancy. In a similar manner, a sea-level curve for MIS 6/5e was constructed from Huon Peninsula data. Four distinct oscillations in sea level are implied (Fig. 5D), agreeing reasonably well with our record, particularly considering the uncertainty of single-point maxima in the Huon record. The major reversal of sea level during the MIS 6/5 transition is very similar to the interpretation of the original investigators (*19*), based on uncorrected ages, but the timing is slightly different. Our curve is also in good general agreement with previous sea-level interpretations from carefully screened conventional ages (Fig. 5E) but resolves much more detail. These differences may be crucial for those using sea-level curves to interpret other data, such as studies of ocean salinity (*20*) or primate evolution (*21*). The agreement of our Barbados record with sea-level records from around the globe suggests that detailed sea-level changes can be resolved with confidence.

Although it is probable that further work will result in revisions of the detailed sea-level curve presented here, the record as a whole strongly suggests that suborbital variability is a persistent feature of the record during both glacial and interglacial periods. This variability falls into a broad suborbital band, with second-order highstands occurring every 3 to 9 ky. Similar variability, observed in $\delta^{18}O$ records from the Atlantic and Pacific (*22*, *23*), has been attributed to changes in sea level (*23*), and our results support this idea. With amplitudes of 6 to 30 m, inferred rates of change approach 10 m per 1000 years, surpassing estimates of the current rate of sea-level rise (*24*) and approximating the average rate of the most recent deglaciation. Although some coral records suggest suborbital fluctuations for parts of MIS 3 and MIS 5 (*8*, *9*, *19*, *25*, *26*), our high-resolution record indicates that this variability persists throughout MIS 5, MIS 6, and MIS 7. Suborbital sea-level variability during glacial periods has been linked to ice-sheet dynamics (*7*, *8*). If interglacial variability is to be attributed to the same cause, it suggests instability in the remaining ice sheets

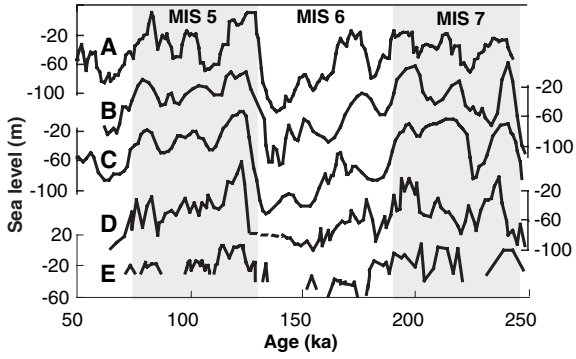

Fig. 3. A comparison of five sea-level records, each on its own time scale. (**A**) Sea-level estimates derived from the Vostok atmospheric $\delta^{18}O$ record and a marine $\delta^{18}O$ record (*29*). (**B**) Sea-level estimates from marine $\delta^{18}O$ data, corrected for temperature with Mg/Ca ratios (*30*). (**C**) Sea-level estimates from $\delta^{18}O$ using regression analysis of coral sea-level and $\delta^{18}O$ data (*31*). (**D**) Sea-level estimates from Red Sea salinity (*6*). (**E**) The coral sea-level record from this work.

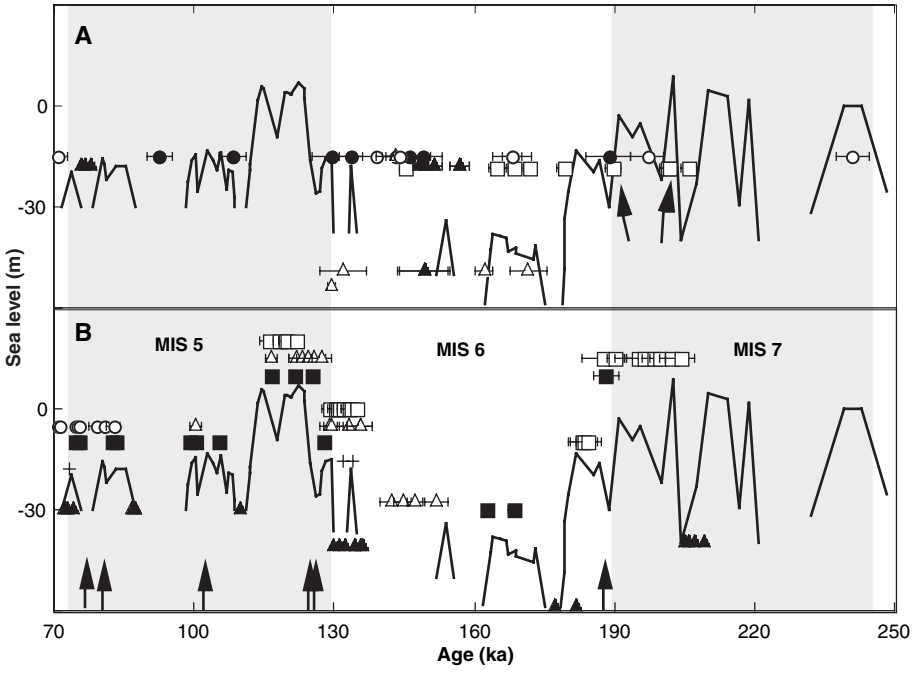

Fig. 4. A comparison of our high-resolution sea-level record (solid line) with the U/Th ages and elevations of speleothem deposits. (**A**) Speleothem sea-level constraints (*32*). Open squares are from (*33*), solid circles from (*34*), open triangles from (*35*), solid triangles from (*36*), and open circles from (*37*). The growth of the speleothems indicates that sea level must have been below the elevation of the cave. Therefore, data points should plot above the sea-level curve (*38*). Arrows indicate ages bracketing marine crust in the record of (*33*). (**B**) Speleothem climate indicators. Warm climate indicators are plotted above the sea-level curve and cold climate indicators below. Speleothem growth indicating warm and/or wet climate: Open squares are from (*39*), solid squares from (*40*), open circles from (*41*), and open triangles from (*42*). Physically observed hiatuses (arrows) suggest cold and dry climate. Spelothem growth indicating cold climate is from (*43*); solid triangles indicate growth ages and crosses indicate short hiatuses, suggesting brief warming.

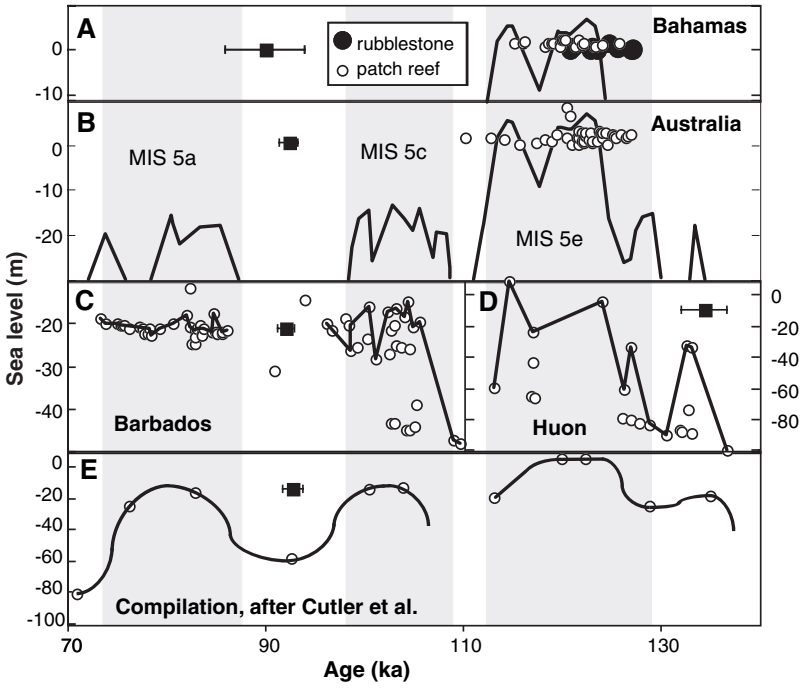

Fig. 5. A comparison of our sea-level record with other coral data (*32*). (**A**) Last Interglacial sea level from open-system ages of Bahamas corals, from isotope ratio data of (*44*). The solid line is our sea-level curve from Fig. 2. (**B**) Last Interglacial sea level from open-system ages of Australian corals, from isotope ratio data of (*45, 46*). Solid lines are our sea-level curves from Fig. 2. (**C**) A relative sea-level curve for MIS 5a and MIS 5c from open-system ages of Barbados corals, from isotope ratio data of (*9*). Solid line is the inferred sea-level change. (**D**) A relative sea-level curve for MIS 6/5 from open-system ages of Huon Peninsula corals, from isotope ratio data of (*19, 47*). Solid line is the inferred sea-level change. (**E**) Sea-level interpretation of (*48*) from a compilation of carefully screened conventional coral ages from Barbados, the Bahamas, and the Huon Peninsula. Solid lines are the sea-level interpretations of (*48*). The solid square symbol in each panel indicates the typical age precision for each data set.

of the far Northern Hemisphere and Antarctica. If substantial sea-level variability is a common feature of previous interglacials, why is there a lack of evidence of similar variations during the Holocene? One difference between the present interglacial and the previous interglacials of MIS 5 and MIS 7 is the modern orbital configuration: The amplitude of the precession cycle is much weaker during the Holocene because of a low in the 413-ky eccentricity cycle. If this is the cause of Holocene sea-level stability, it suggests that orbital configuration plays some role in modulating suborbital sea-level variability.

This study highlights the potential of open-system ages for substantially improving the resolution and accuracy of coral sea-level reconstructions. The ability to generate detailed records from multiple locations is an important strength of this approach, providing a cross-check against stratigraphic complications such as slumping, faulting, differences in coral growth depth, and corals in apparent growth positions that have actually been transported from their original elevations.

References and Notes

1. M. M. Milankovitch, *Serb. Acad. Beorg. Spec. Pub.* **132** (1941).
2. J. D. Hays, J. Imbrie, N. J. Shackleton, *Science* **194**, 1121 (1976).
3. K. J. Mesolella, R. K. Matthews, W. S. Broecker, D. L. Thurber, *J. Geol.* **77**, 250 (1969).
4. W. Dansgaard *et al.*, *Nature* **364**, 218 (1993).
5. W. G. Thompson, M. W. Spiegelman, S. L. Goldstein, R. C. Speed, *Earth Planet. Sci. Lett.* **210**, 365 (2003).
6. M. Siddall *et al.*, *Nature* **423**, 853 (2003).
7. Y. Yokoyama, T. M. Esat, K. Lambeck, *Earth Planet. Sci. Lett.* **193**, 579 (2001).
8. J. Chappell, *Quat. Sci. Rev.* **21**, 1229 (2002).
9. E.-K. Potter *et al.*, *Earth Planet. Sci. Lett.* **225**, 191 (2004).
10. G. Schellmann, U. Radtke, *Earth Sci. Rev.* **64**, 157 (2004).
11. W. S. Broecker, *J. Geophys. Res.* **68**, 2817 (1963).
12. C. Fruijtier, T. Elliot, W. Schlager, *Geol. Soc. Am. Bull.* **112**, 267 (2000).
13. C. D. Gallup, R. L. Edwards, R. G. Johnson, *Science* **263**, 796 (1994).
14. G. M. Henderson, N. C. Slowey, *Nature* **404**, 61 (2000).
15. Materials and methods are available as supporting material on *Science* Online.
16. C. D. Gallup, H. Cheng, F. W. Taylor, R. L. Edwards, *Science* **295**, 310 (2002).
17. R. C. Speed, H. Cheng, *Geol. Soc. Am. Bull.* **116**, 219 (2004).
18. D. A. Richards, J. A. Dorale, in *Uranium-Series Geochemistry*, B. Bourdon, G. M. Henderson, C. C. Lundstrom, S. P. Turner, Eds. (Mineralogical Society of America and Geochemical Society, Washington, DC, 2003), vol. 52, pp. 407–460.
19. T. M. Esat, M. T. McCulloch, J. Chappel, B. Pillans, A. Omura, *Science* **283**, 197 (1999).
20. M. W. Schmidt, H. W. Spero, D. W. Lea, *Nature* **428**, 160 (2004).
21. C. Abegg, B. Thierry, *Biol. J. Linn. Soc.* **75**, 555 (2002).
22. D. W. Oppo, L. D. Keigwin, J. F. McManus, *Paleoceanography* **16**, 280 (2001).
23. D. W. Oppo, B. K. Linsley, Y. Rosenthal, S. Dannenmann, L. Beaufort, *Geochem. Geophys. Geosyst.* **4**, 1001 (2003).
24. S. J. Holgate, P. L. Woodworth, *Geophys. Res. Lett.* **31**, L07305 (2004).
25. K. Sasaki, A. Omura, K. Murakami, N. Sagawa, T. Nakamori, *Quat. Int.* **120**, 51 (2004).
26. E.-K. Potter, K. Lambeck, *Earth Planet. Sci. Lett.* **217**, 171 (2004).
27. C. H. Stirling *et al.*, *Science* **291**, 290 (2001).
28. D. G. Martinson *et al.*, *Quat. Res.* **27**, 1 (1987).
29. N. J. Shackleton, *Science* **289**, 1897 (2000).
30. D. W. Lea, P. A. Martin, D. K. Pak, H. J. Spero, *Quat. Sci. Rev.* **21**, 283 (2002).
31. C. Waelbroeck *et al.*, *Quat. Sci. Rev.* **21**, 295 (2002).
32. The comparison of sea levels from different locations around the globe must be treated with some caution because of global isostatic effects from the loading and unloading of ice over glacial/interglacial cycles. However, comparison of the frequency of suborbital sea-level oscillations in relative sea-level curves should be valid.
33. E. Bard, F. Antonioli, S. Silenzi, *Earth Planet. Sci. Lett.* **196**, 135 (2002).
34. J. Lundberg, D. C. Ford, *Quat. Sci. Rev.* **13**, 1 (1994).
35. P. L. Smart, D. A. Richards, R. L. Edwards, *Cave Karst Sci.* **25**, 67 (1998).
36. D. A. Richards, P. L. Smart, R. L. Edwards, *Nature* **36**, 357 (1994).
37. W.-X. Li *et al.*, *Nature* **339**, 534 (1989).
38. Several investigators have assumed continuous speleothem growth between dated samples. Although the presence of a visible hiatus is proof positive of a discontinuity in the record, the absence of such a hiatus is not evidence of continuous growth. The potential for large hiatuses to escape visual detection is illustrated by the variable preservation of the white biogenic crust marking the 10-ky MIS 7.1 hiatus in the speleothem of (*33*). This crust pinches out laterally along the growth layer, leaving a single growth lamina of ~1 mm that looks very much like sections of the speleothem that are assumed to represent continuous growth. Such a hiatus, particularly one of shorter duration, could not be detected without much closer spacing of dated samples.
39. C. Spotl, A. Mangini, N. Frank, R. Eichstadter, S. J. Burns, *Geology* **30**, 815 (2002).
40. V. Planges, C. Causse, D. Genty, M. Paterne, D. Blamart, *Earth Planet. Sci. Lett.* **201**, 87 (2002).
41. D. Genty *et al.*, *Nature* **421**, 833 (2003).
42. J.-x. Zhao, Q. Xia, K. D. Collerson, *Earth Planet. Sci. Lett.* **184**, 635 (2001).
43. X. Wang *et al.*, *Nature* **432**, 740 (2004).
44. J. H. Chen, H. A. Curran, B. White, G. J. Wasserburg, *Geol. Soc. Am. Bull.* **103**, 82 (1991).
45. C. H. Stirling, T. M. Esat, M. T. McCulloch, K. Lambeck, *Earth Planet. Sci. Lett.* **135**, 115 (1995).
46. C. H. Stirling, T. M. Esat, K. Lambeck, M. T. McCulloch, *Earth Planet. Sci. Lett.* **160**, 115 (1998).
47. M. Stein *et al.*, *Geochim. Cosmochim. Acta* **57**, 2541 (1993).
48. K. B. Cutler *et al.*, *Earth Planet. Sci. Lett.* **206**, 253 (2003).

49. We thank W. Broecker, G. Henderson, and S. Hemming for many productive discussions and M. Stein and the late R. Speed for guidance and debate in the field. McGill University's Bellairs Research Institute of Barbados provided logistical support. Grants from the Lamont Climate Center, the Comer Science & Educational Foundation, and the Goodfriend Prize and start-up funds from LDEO and Columbia University for S.L.G. supported this work. The LDEO Deep-Sea Sample Repository curated some of the corals used for this sea-level reconstruction. Support for this facility is provided by NSF (grant OCE00-02380) and the Office of Naval Research (grant N00014-02-1-0073). This is LDEO contribution no. 6745.

Supporting Online Material

www.sciencemag.org/cgi/content/full/308/5720/401/DC1
Materials and Methods
Fig. S1
Table S1
References

13 August 2004; accepted 3 March 2005
10.1126/science.1104035